P4.62   **EXAMINATION OF WSR-88D VWP DATA IN PROXIMITY TO STRONG TORNADOES**

Jared L. Guyer * and John A. Hart
NOAA/NWS Storm Prediction Center, Norman, Oklahoma

1. INTRODUCTION

Among other factors, it is well-established that influences of at least sufficiently strong shear and storm relative helicity (SRH) within the lowest few km AGL are key ingredients with respect to supercells that tend to produce tornadoes. Observationally monitoring and evaluating temporal trends and relatively fine-scale changes of low-level shear and SRH are critically important to operational forecasters at the Storm Prediction Center (SPC) and other National Weather Service (NWS) offices.

One method for monitoring such low-level wind changes can be done through means such as the Weather Surveillance Radar-1988 Doppler (WSR-88D) network derived velocity azimuth display (VAD) wind profile (VWP). VWP data from WSR-88Ds offer much greater temporal and spatial observational density as compared to observed rawinsondes (typically only twice a day) and wind profilers (mainly central United States and recently decreasing in number). Wind information is processed by the WSR-88D VAD algorithm and if sufficient data reliability exists (symmetry and lack of statistical error), the VWP displays areal-averaged horizontal winds on a time versus height basis for each radar volume scan when sufficient scatterers are available (Klazura and Imy 1993). Stensrud et al. (1990) found VAD wind data to be comparable to a digital sounding system except when winds were weak. A number of other studies have discussed possible VWP biases and contamination issues from migratory birds and fronts (e.g. Niziol 1998; Gauthreaux et al. 1998) along with other potential errors and discrepancies (Nelson et al. 1995). While VWP data may be subject to reliability uncertainty and associated caveats (as any dataset), available VWP data (for which sufficient scatterers existed) were used in this study on an as-is basis, especially given its operational availability and, oftentimes, lack of pseudo real-time alternatives.

A number of past studies have used proximity rawinsonde data (Davies and Johns 1993; Craven and Brooks 2004) and model-based (e.g., RUC; Thompson et al. 2003) information to estimate supercell tornado environments, but relatively fewer aggregate tornado studies have utilized WSR-88D VWP information to evaluate vertical wind shear associated with tornadoes. Medlin and Bunkers

(2008) examined the wind shear characteristics prior to tornadoes along the north-central Gulf Coast using WSR-88D VWP data from a singular radar (KMOB).

In this study, a multi-year (2008-2011) WSR-88D VWP dataset was used to examine the magnitude and temporal trends of low-level shear and SRH associated with strong tornado environments. Of particular focus are observed supercells that produced strong tornadoes (defined here as EF3 and greater) within close proximity (≤75 km) of a contiguous United States (CONUS) WSR-88D site. This WSR-88D VWP-based analysis provides additional observationally-based examination of the low-level wind profiles associated with the near-storm environments of strong tornadoes.

2. DATA COLLECTION AND METHODOLOGY

With a study emphasis on strong and violent tornadoes in close proximity to CONUS WSR-88D locations, tornado statistics for EF3-EF5 tornadoes were utilized from the *Storm Data*-derived ONETOR database from parts of a four-year period (May 2008-December 2011). The tornado database was filtered to those EF3+ tornadoes that occurred ≤75 km from any CONUS WSR-88D location at any point of the tornado track path for the period of study. Upon evaluation of archive level II volumetric Doppler radar data (in a manner similar to Smith et al. 2012), only tornado tracks associated with discrete, semi-discrete, or clusters of supercells were utilized, with a relatively small number (7 cases) of squall line and QLCS related tornadoes excluded.

For this study, observed wind profiles for 0-6 hours prior to tornado occurrence were derived from an archive of WSR-88D VWP data. Proximity surface wind observations (ASOS/AWOS) within the uncontaminated inflow side of the storm were used to augment the lowest level of the observed WSR-88D VWP data, typically from a time 0-0.5 hour prior to tornado onset. Radar observed storm motions were utilized for SRH calculations. Ultimately, time-height series of VWP data and associated vertical shear calculations were constructed for each tornado event, such as in Fig. 1 for 10 May 2010 in central Oklahoma.

_____

* *Corresponding author address*: Jared L. Guyer
NOAA/NWS Storm Prediction Center, National Weather Center, 120 David L. Boren Blvd, Suite 2300, Norman, OK 73072; e-mail: Jared.Guyer@noaa.gov
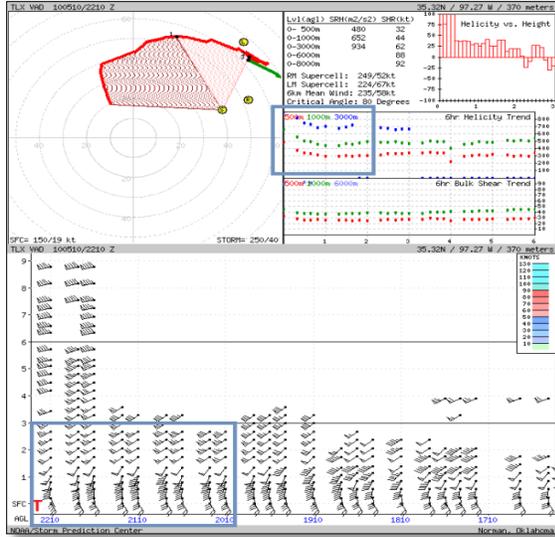
Figure 1. Hodograph and time-height display (6-hr trend with most recent data on left side) from KTLX (Oklahoma City/Twin Lakes) VWP ending at 2210 UTC 10 May, 2010. Approximate tornado time denoted by a red T. Increase in low-level SRH highlighted by blue rectangles. Observed storm motion used for SRH calculations.

48 Total Tornadoes	EF-Scale	# Tornadoes
	EF3	29
	EF4	16
	EF5	3

Table 1. Tornadoes included in this study by EF-Scale.
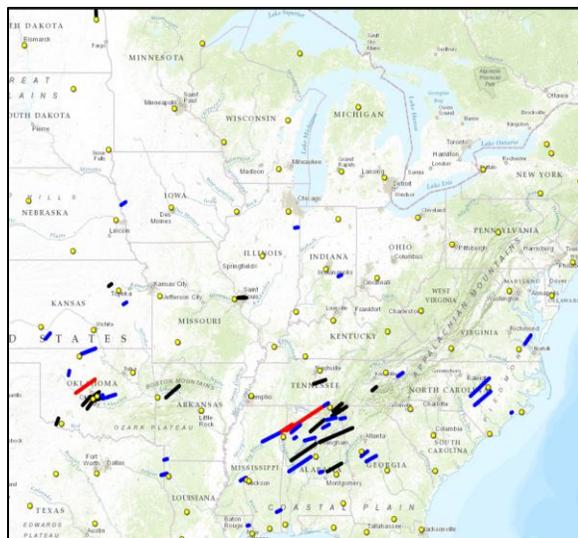
Figure 2. Map of EF3-EF5 tornado tracks (2008-2011) ≤75 km of NEXRAD WSR-88D radar site. EF3 tornado tracks in blue, EF4 tornadoes in black, and EF5 tornadoes in red. WSR-88D radar locations noted by yellow circles.

3. TORNADO DATASET

Out of 182 CONUS EF3+ tornado tracks (May 2008-December 2011), a total of 48 EF3+ tornadoes (Table 1) were found to satisfy the ≤75 km WSR-88D proximity criteria for which Level II radar data was available. These 48 tornadoes occurred on 18 separate convective days (i.e., 12 UTC - 12 UTC) in parts of the Great Plains, southeast United States, and Midwest (Fig. 2). It should be noted that the cases are dominated by several significant tornado days including prolific outbreaks on 24 May 2011, 16 April 2011, and especially 27 April 2011 (15 of 48 events; Table 2). The tornado dataset was largely comprised (96%) of springtime events (April to mid-June), with only two cool season cases (one each in November and January). Regarding the time of day, tornado onset times spanned from 17:19 UTC to 4:53 UTC, although most occurred in the mid/late afternoon and early/mid evening hours (83% between 20 UTC and 04 UTC).

Date	WSR-88D Location
5/23/08	KDDC
6/03/08	KIND
6/11/08	KTWX KOAX
4/09/09	KSHV
4/10/09	KOHX KHTX
1/20/10	KSHV
4/24/10	KHTX(2) KBMX
5/10/10	KTLX(4) KVNX
6/05/10	KLOT
6/17/10	KMVX
4/15/11	KMOB KBMX
4/16/11	KRAX(2) KAKQ KMHX
4/22/11	KLSX
4/27/11	KHTX(4) KGWX(4) KBMX(3) KMRX(2) KFFC(2)
5/21/11	KTWX
5/24/11	KTLX(3) KSRX KVNX
5/26/11	KLIX
11/7/11	KFDR

Table 2. WSR-88D locations used by identifier (accompanying numbers represent number of tornadoes if more than one) by convective day (12 UTC) for tornadoes (EF3-EF5) examined in this study.

4. ANALYSIS

Not surprisingly, WSR-88D VWP derived hodographs for the EF3+ tornado events typically exhibited an elongated clockwise-curving low-level hodograph character. Resultant very strong low-level shear and SRH are consistent with prior studies of strong to violent tornado environments (Thompson et al. 2003; Cohen 2010). In this study, mean bulk shear magnitude for 0-0.5 km, 0-1 km, and 0-3 km AGL were 25 kt, 36 kt, and 54 kt, respectively (Fig. 3).

Mean SRH values for 0-0.5 km, 0-1 km, and 0-3 km AGL were 216 m^2/s^2, 341 m^2/s^2 and 502 m^2/s^2, respectively (Fig. 4). Given these values, the ratio for 0-1 km mean SRH vs. 0-3 km mean SRH was found to be 69%, which is indicative of a relatively high near-ground concentration of SRH for EF3+ tornadoes. These findings are relatively similar to Cohen 2010 (albeit EF4+ tornadoes vs. EF3+ tornadoes in this study). In fact, our findings show that the lowest 0.5 km layer AGL accounted for 64% of 0-1 km SRH and 45% of 0-3 km SRH on average for EF3+ tornadoes (Fig. 5). In terms of bulk shear magnitude, the 0-0.5 km layer AGL bulk shear was 69% of the 0-1 km mean bulk shear magnitude and 46% of the 0-3 km mean bulk shear magnitude (not shown).
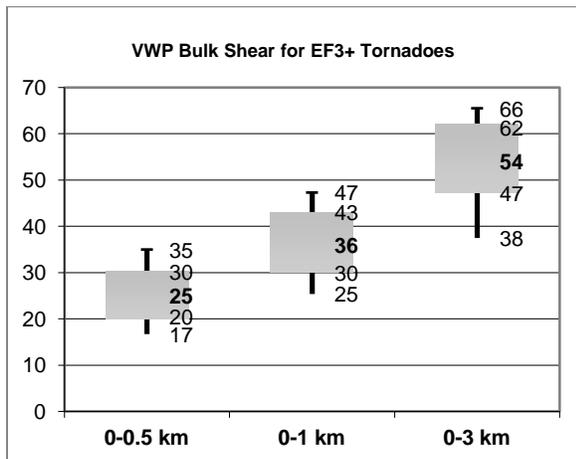
Figure 3. Box and whisker diagrams of low-level (0-0.5, 0-1, & 0-3 km AGL) bulk shear (kt) for EF3+ tornadoes ≤75 km of WSR-88D VWP for 2008-2011. Each box is representative of the 25th to 75th percentiles of values with the *mean* value in the middle. The outer whiskers represent the 10th and 90th percentiles.

Additionally, relatively short-term temporal trends of low-level bulk shear and SRH preceding tornado development were examined. It was found that 0-0.5 km and 0-1 km SRH increased (at least modestly) over the preceding 1-2 hours prior to tornado development in 47% of cases, while increases in 0-0.5 km and 0-1 km bulk shear magnitude occurred in 61% of cases (such as Fig. 1 in both regards). Even though the overall magnitudes were typically very strong, short-term increasing trends were less evident within the 0-3 km layer (e.g. 0-3 km bulk shear increased in the tornado-preceding 1-2 hours only 42% of the time).

Prior studies such as Thompson and Edwards (2000) and Miller (2006) discussed low-level hodograph characteristics of strong tornadoes including an observationally prominent low-level (1-1.5 km and below) "sickle" shape. Esterheld and
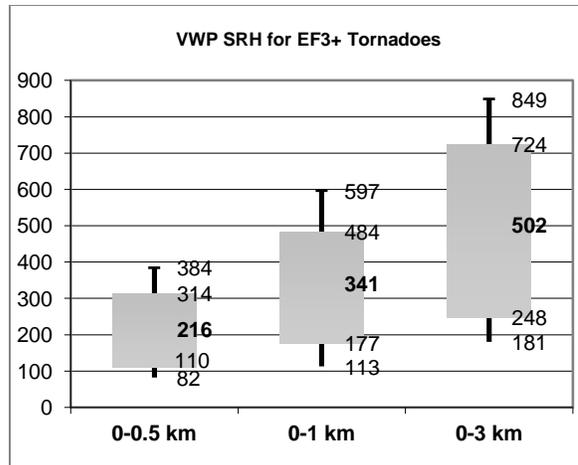
Figure 4. Same as Fig. 3, except 0-0.5 km SRH, 0-1 km SRH, and 0-3 km SRH (m^2/s^2).
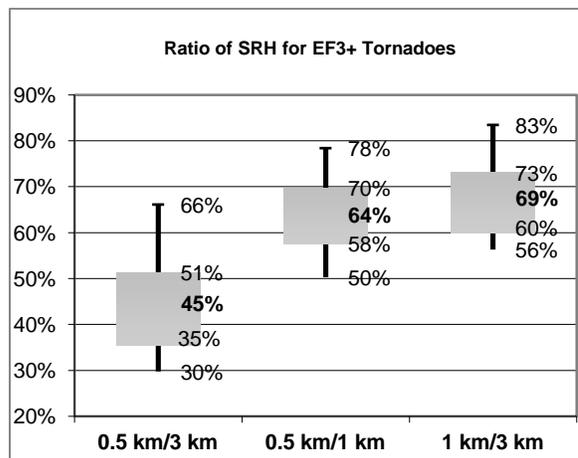
Figure 5. Same as Fig. 3, except ratio of 0-0.5 km SRH to 0-3 km SRH, 0-0.5 km SRH to 0-1 km SRH, and 0-1 km SRH to 0-3 km SRH (m^2/s^2).

Guiliano (2008) examined this hodograph kink in greater detail for tornado cases in Oklahoma. They found that the "critical angle" (defined as the angle between the storm-relative inflow vector at 10 m and the 10-500 m AGL shear vector) tended to be near 90 degrees, particularly for supercell that produced (E)F2+ tornadoes. Relatively similar to the findings of Esterheld and Guiliano (2008), our more spatially diverse study found that the median critical angle to be 79 degrees with the interquartile critical angle values ranging from 63 to 88 degrees (Fig. 6). Our preliminary case analysis reflected a greater tendency for near-90 degree angles strong tornado cases in the Plains, while a number of strong or violent tornadoes in the southeast U.S. (such as 27 April 2011) occurred in association with a critical angle far less than 90 degrees (e.g., ~55-60 degrees in some cases).

Critical Angle for EF3+ Tornadoes

```
100
 90          ┬ 97
             88
 80          77
 70
             63
 60          ┴ 55
 50
 40
```
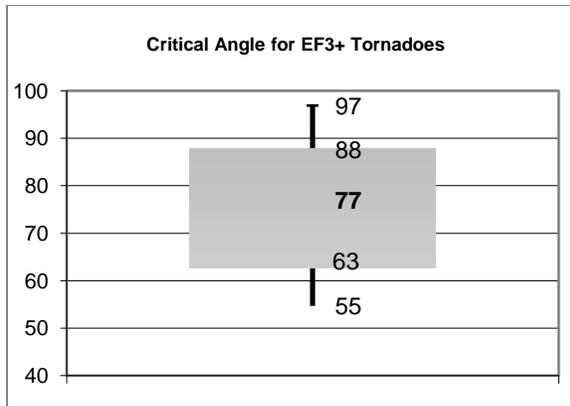
Figure 6. Same as Fig. 3, except Critical Angle in degrees (Esterheld and Giuliano 2008).

5. COMPARISON TO SPC ENVIRONMENT DATABASE

As a supplement to direct observational data, an objective analysis (SFCOA) based on a blend of surface METAR observations and RUC (now RAP) analysis fields (Bothwell et al. 2002) is heavily utilized by Storm Prediction Center (SPC) forecasters and NWS field personnel for monitoring environmental changes on an hourly basis. As such, a comparison of the VWP data to SFCOA was an appropriate step to investigate potential differences that may be evident between these datasets. Accordingly, comparisons were made to estimated tornado environment information from a gridded SPC database as described by Dean et al. (2006). Within this database, severe storm reports are objectively linked to estimated environments as derived from hourly SFCOA grids (40 km grid length). Specific environmental parameters (e.g., 0-1 SRH, etc.) were objectively derived from the 40 km grid box in which each EF3+ tornado event occurred.

In aggregate for the 48 EF3+ tornado cases, our preliminary findings were that WSR-88D derived 0-1 km bulk shear (Fig. 7) and 0-1 km SRH (Fig. 8) tended to be slightly lower (63% of the time) as compared to the gridded SFCOA data. The mean absolute difference was 7 kt for 0-1 km bulk shear magnitude and 187 m^2/s^2 for 0-1 km SRH. However, it is important to note that case-to-case variability was considerable when comparing WSR-88D VWP data and the SFCOA. In 27% of the EF3+ tornado cases, WSR-88D VWP derived 0-1 km shear magnitude was found to vary by more than 10 kt from SFCOA (WSR-88D VWP was lower for 62% of these cases). In 54% of the tornado cases, WSR-88D VWP derived 0-1 km SRH was found to vary by more than 150 m^2/s^2 from SFCOA (WSR-88D VWP was lower for 77%). Aside from storm motion inconsistencies (forecast vs. observed) between the datasets for calculating SRH, some of the differences may also be attributable to the gridded nature of the SFCOA comparative dataset. Regardless, such differences stress the critical case-by-case importance of observational

based monitoring of near-storm environment information and evaluation of storm motion by operational forecasters.

0-1 km Bulk Shear for EF3+ Tornadoes

```
60
                                        ┬ 53
50          ┬ 47                        48
             43
40          36                          39
             30                         29
            ┴ 25                        ┴ 25
30
20
      WSR-88D VWP              SFCOA
```
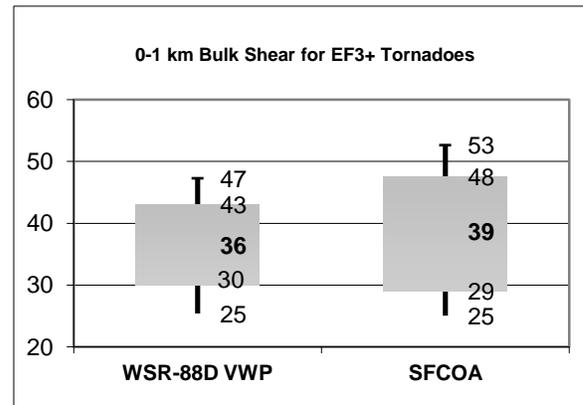
Figure 7. Same as Fig. 3, except a comparison of 0-1 km bulk shear (km) for WSR-88D VWP vs. SPC objective mesoanalysis (SFCOA).

0-1 km SRH for EF3+ Tornadoes

```
800
700                                     ┬ 675
600         ┬ 597
500          484                        539
400          341                        438
300                                     344
200          177                        199
100         ┴ 113
  0
      WSR-88D VWP              SFCOA
```
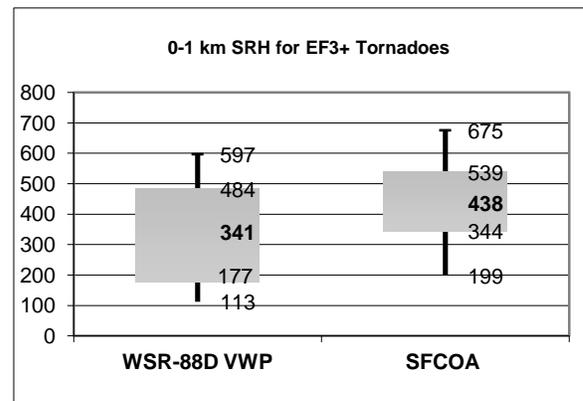
Figure 8. Same as Fig. 3, except a comparison of 0-1 km SRH (m^2/s^2) for WSR-88D VWP vs. SPC objective mesoanalysis (SFCOA).

6. SUMMARY AND FUTURE WORK

This study examined low-level shear calculated from WSR-88D VWP data associated with 48 EF3+ tornadoes that occurred in close spatial proximity to CONUS WSR-88D sites. Compared to the relative prevalence of prior studies using platforms such as observed rawinsonde data, profiler network, and/or numerical models (e.g. RUC), WSR-88D VWP data may be an underutilized resource, especially given its spatiotemporal availability and operational utility in severe local storm environments. This preliminary study found that WSR-88D VWP-derived values of low-level shear and SRH were very large (e.g., mean 0-1 km SRH of 341 m^2/s^2) in association with EF3+ tornadoes, with a trend toward increasing low-level shear/SRH within the 0-0.5 km and 0-1 km layers in roughly half of the cases during the 1-2 hours prior to tornado onset.

It should again be acknowledged that these preliminary results and conclusions are derived from a relatively limited dataset of tornado events that are dominated by several high-end outbreak days. Future work will include the addition of EF1 and EF2 tornado cases ≤75 km of a CONUS WSR-88D, along with more comprehensive examinations of the fine-scale variability and pre-storm low-level wind shear trends for supercells associated with strong to violent tornadoes. Comparisons and sensitivity tests will also be made to observed rawinsonde and wind profiler network data.

7. REFERENCES

Bothwell, P. D., J. A. Hart, and R. L. Thompson, 2002: An integrated three-dimensional objective analysis scheme in use at the Storm Prediction Center. Preprints, 21st Conf. on Severe Local Storms, San Antonio, TX, Amer. Meteor. Soc., J117–J120.

Cohen, A. E., 2010: Indices of violent tornado environments. Electronic J. Operational Meteor., 11 (6), 1-24.

Craven, J. P., and H. E. Brooks, 2004: Baseline climatology of sounding derived parameters associated with deep moist convection. Natl. Wea. Dig., 28, 13-24.

Davies, J. M., and R. H. Johns, 1993: Some wind and instability parameters associated with strong and violent tornadoes. 1. Wind shear and helicity. The Tornado: Its Structure, Dynamics, Prediction, and Hazards, Geophys. Monogr., No. 79, Amer. Geophys. Union, 573–582.

Dean, A.R., R.S. Schneider, and J.T. Schaefer, 2006: Development of a Comprehensive Severe Weather Forecast Verification System at the Storm Prediction Center. Preprints, 23nd Conf. Severe Local Storms, St. Louis MO.

Esterheld, J. M. and D. J. Giuliano, 2008: Discriminating between tornadic and non-tornadic supercells: A new hodograph technique. *Electronic J. Severe Storms Meteor.*, 3 (2), 1-50.

Gauthreaux, S. A., Jr., D. S. Miszahi, and C. G. Belser, 1998: Bird migration and bias of WSR-88D wind estimates. Wea. Forecasting,13, 465–481.

Klazura, G. E., and D. A. Imy, 1993: A description of the initial set of analysis products available from the NEXRAD WSR-88D system. Bull. Amer. Meteor. Soc., 74, 1293–1311.

Medlin, J.M., and M. Bunkers, 2008: An Examination of North Central Gulf Coast Cold Season Pre-Tornadic Vertical Wind Shear Environments since 1996. Presented at 33rd National Weather Association Annual Meeting, Louisville, KY.

Miller, D. J., 2006: Observations of low level thermodynamic and wind shear profiles on significant tornado days. Preprints, *23rd Conf. on Severe Local Storms,* St. Louis, MO, Amer. Meteor. Soc., 1206-1223.

Nelson, S., F. Carr, and L. Ruthi, 1995: Intercomparison of horizontal velocities observed by modern wind-finding systems.. Preprints, 9th Symposium on Meteorological Observations and Instrumentation, Charlotte, NC, AMS, 5 pp.

Niziol, T. A., 1998: Contamination of WSR-88D VAD Winds Due to Bird Migration: A Case Study. Eastern Region WSR-88D Operations Note No. 12, August, 1998.

Smith, B. T., R. L. Thompson, J. S. Grams, C. Broyles, H E. Brooks, 2012: Convective Modes for Significant Severe Thunderstorms in the Contiguous United States. Part I: Storm Classification and Climatology. Wea. Forecasting, 27, 1114–1135.

Stensrud, D. J., M. H. Jain, K. W. Howard, R. A. Maddox, 1990: Operational Systems for Observing the Lower Atmosphere: Importance of Data Sampling and Archival Procedures. *J. Atmos. Oceanic Technol.*, 7, 930–937.

Thompson, R. L., R. Edwards, 2000: An Overview of Environmental Conditions and Forecast Implications of the 3 May 1999 Tornado Outbreak. Wea. Forecasting, 15, 682–699.

Thompson, R. L., R. Edwards, J.A. Hart, K.L. Elmore and P.M. Markowski, 2003: Close proximity soundings within supercell environments obtained from the Rapid Update Cycle. Wea. Forecasting, 18, 1243-1261.